New Materials, Compounds and Applications
Vol.8, No.3, 2024, pp.422-429
https://doi.org/10.62476/nmca83422

HAFNIUM DIBORIDE: A NOTABLE SOLID-STATE MATERIAL FOR EFFICIENT PHOTOTHERMAL CONVERSION

Reeja Gopalakrishnan Nair[1], Ashalatha A.[2], Anupama M.[3*]

[1]Department of Physics, Government College Malappuram, Kerala, India
[2]Department of Chemistry, S.N. College Chempazhanthy, Thiruvananthapuram, Kerala, India
[3]Department of Physics, N.S.S. College, Manjeri, Malappuram, Kerala, India

Abstract. We report the remarkable light-to-heat conversion observed in commercially available, ready-to-use bulk hafnium diboride (HfB_2) powder, which exhibits strong wide-spectrum absorption and minimal photoluminescence. 100 mg of the powder sample, uniformly spread on an aluminium foil, was subjected to continuous-wave, blue laser irradiation and the rise in sample temperature was measured using a K - type thermocouple. The bulk HfB_2 powder sample showed substantial photothermal conversion and displayed exceptional thermal, chemical and photo-stability under diverse irradiation conditions. Furthermore, the photothermal effect proved to be highly reproducible, highlighting the suitability of HfB_2 powder for a range of industrial applications.

Keywords: *Hafnium diboride, broadband absorption, non-radiative relaxation, photothermal conversion.*

Corresponding Author: *Anupama M., Department of Physics, N.S.S. College, Manjeri, Malappuram, Kerala, India, Tel.: 09946518547, e-mail: anupamarajeesh84@gmail.com*

Received: *11 September 2024;* ***Accepted:*** *30 November 2024;* ***Published:*** *10 December 2024.*

1. Introduction

The photothermal effect has showcased its effectiveness in a wide array of applications, spanning from bioimaging, cancer therapy and drug delivery to microfluid heating, material synthesis and driving chemical reactions with high activation energies (Huang & El-Sayed, 2011; Kim *et al*., 2019; Liu *et al*., 2021; Walsh *et al*., 2015). This mechanism is a highly intriguing light-matter interaction where material systems transform a substantial amount of radiant light to heat. When photons interact with matter, electron excitation takes place by photon absorption. These excited electrons being unstable, subsequently de-excite via radiative or non-radiative pathways. In several materials, non-radiative relaxation dominates, displaying direct conversion of the absorbed optical energy to heat, categorizing them as photothermal agents (Zhang *et al*., 2024). Ideally, a photothermal material should demonstrate robust optical absorption, effective heat conduction, minimal heat emission, negligible photoluminescence and exceptional optical, thermal and chemical stability (John *et al*., 2017; Johnson *et al*., 2015). In addition, the ability for broad-spectrum absorption is also a critical attribute that facilitates efficient harvesting of renewable solar energy through the photothermal

How to cite (APA):
Reeja, G.N., Ashalatha, A., & Anupama, M. (2024). Hafnium diboride: A notable solid-state material for efficient photothermal conversion. *New Materials, Compounds and Applications, 8*(3), 422-429 https://doi.org/10.62476/nmca83422

transduction process (Hong *et al*., 2022; Wu *et al*., 2019; Yao *et al*., 2018). Over the past few years, a multitude of plasmonic metals, semiconductors, carbon-based systems and polymer based organic molecules have been identified as photothermal agents, especially in their low-dimensional configurations like nanosheets (2D), quantum dots (0D), nanofluids etc. (Chen *et al*., 2016; Cheng *et al*., 2022; Huang *et al*., 2017; Huang & El-Sayed, 2010; Jiang *et al*., 2013; Yu *et al*., 2020; Zhou *et al*., 2022). This focus on nanostructures is primarily because specialized properties like Localised Surface Plasmon Resonance, which significantly boosts optical absorption, particularly in noble metal nanoparticles, that correlates directly with photothermal transduction are notably pronounced within the nano regime (Huang & El-Sayed, 2010). Moreover, the heat generated by nanoscale systems can be precisely controlled both in the spatial and temporal dimensions enabling their utilization for numerous therapeutic applications (Johnson *et al*., 2015). However, exposure to intense irradiation causes these nanoparticles to undergo changes like melting, fragmentation and aggregation which adversely affects the spatial and temporal distribution, as well as the magnitude of heat generated via the photothermal effect. This, in turn, limits the advantage of using nanoparticles for meticulously controlling local heat in biological applications and for driving high-barrier chemical reactions (Huang *et al*., 2010; Johnson *et al*., 2015). Furthermore, in a typical photothermal transduction experiment using nanosized photothermal agents, the nanoparticles are dispersed in appropriate solvents or matrices such as polymers before irradiation. This often necessitates the use of surfactants or other stabilizing reagents whose temperature-dependant stability, phase stability and light attenuation properties will also impose restrictions to the photothermal applicability of these materials (Estelrich & Busquets, 2018; Johnson *et al*., 2015; Yamamoto *et al*., 2019). Needless to say, the photothermal agents in their nanoforms need to be synthesized using various fabrication techniques before application. Post-use, it is crucial to develop critical separation methods to prevent their introduction into the environment for avoiding additional health and environmental issues. Retrieving them for sustainable reuse also poses a significant challenge (Salafi *et al*., 2017). All these factors reduce the cost-effectiveness for their large-scale applications. Hence, identifying and employing commercially available, ready-to-use bulk materials that offer intense wide spectrum absorption, minimal photoluminescence, usable in the solid form without requiring surfactants and showing high photo-thermo-chemical stability would be greatly beneficial for enhanced light-to-heat conversion. This approach also eliminates the need for additional synthesis routes or purification steps typically associated with nanostructure fabrication.

Transition metal diborides, including HfB_2, ZrB_2, TiB_2 and TaB_2 have garnered much attention in the recent years due to their superior characteristics like high melting point, good thermal conductivity and mechanical strength (Ma *et al*., 2021). Hafnium Diboride is metal diboride belonging to the class of ultra-high temperature ceramics characterized by very high melting point, excellent electrical and thermal conductivity, hardness and chemical stability making them potentially employable for applications requiring high-temperature resilience above 3000 ^{0}K, such as nose caps, sharp leading edges, vanes and similar objects for use in hypersonic flight, atmospheric re-entry, rocket propulsion, furnace elements, cutting tools and electrodes in Pulsed Laser Deposition (Lawson *et al*., 2011; Wuchina *et al*., 2004; Zhang *et al*., 2008). Their outstanding heat and oxidation resistance along with their thermal stability, has elevated the popularity of

hafnium diboride coatings (Das *et al*., 2023). All these applications utilise the superior thermal and robust mechanical properties of HfB_2 which have been extensively studied.

Till date, HfB_2 remains unexplored in terms of its optical characteristics. Analysis based on previously reported Density functional theory (DFT) computations suggest that HfB_2 has potential as a broad-band optical absorber capable of non-radiative recombinations (Lawson *et al*., 2011; Zhang *et al*., 2008). However, as of yet, HfB_2 has not been identified or demonstrated as a material suitable for photothermal conversion. Building on these insights, our current research underlines the novel application of commercially available polycrystalline HfB_2 bulk powder as a remarkable photothermal agent capable of broad-band absorption, yet, possessing low photoluminescence and outstanding thermal, chemical and optical stability. The purity and morphology of the sample were analyzed and its role as a photothermal agent was confirmed through optical absorption and photoluminescence studies.

2. Experimental

2.1. Materials

Hafnium diboride powder (purity 99%, mesh size-325) was obtained from Sigma Aldrich and was utilised as received without any further alteration or purification.

2.2. Characterisations

The structure and phase purity of bulk HfB_2 powder was investigated by X-ray diffraction employing PANalyticalX'Pert powder diffractometer, set at an operating voltage and current of 45 kV and 40 mA respectively using Cu Kα radiation having a wavelength of 1.5406 Á. The samples were scanned over a 2θ range of 20° to 90° at a scan rate of 0.026°/s. The morphology of the sample was analysed using a Field emission scanning electron microscope (FESEM) (ZEISS Gemini 1 Sigma 300) operating at an accelerating voltage of 3 kV. The specimen for FESEM was prepared by evenly spreading HfB_2 powder on a conductive carbon tape. The optical absorption spectrum of the powder sample was collected using an UV-diffuse reflectance spectrophotometer having an integrating sphere arrangement (Ocean Insight FLAME Scientific-Grade spectrometer, Model: FLAME-UV-VIS-ES, Serial No.FLMT08457), with Barium sulphate ($BaSO_4$) as the reference material. The photoluminescence (PL) spectra of the bulk HfB_2 powder at different excitation wavelengths were obtained using a PerkinElmer LS-55 spectrophotometer.

2.3. Photothermal Experiment

The photo-to-thermal conversion efficiency of bulk HfB_2 powder was evaluated through a detailed experimental procedure. In this setup, 100 mg of the powder sample was uniformly distributed on an aluminum foil, which was then placed in close contact with a K-type thermocouple. The thermocouple was connected to a MAX6675 IC, which included a thermocouple amplifier, a 12-bit digitizer and an SPI communication interface, as well as built-in cold junction compensation circuitry. The MAX6675 IC recorded the temperature at the contact point between the thermocouple and the sample. Prior to conducting the experiment, the thermocouple was calibrated using an ice bath (approximately 0°C) and boiling water (approximately 100°C). A data acquisition device-KuttyPy Plus captured the data from the MAX6675 IC and transferred it through USB to

a PC for analysis. The experimental procedure involved irradiating the sample with a continuous-wave blue laser, which has a wavelength of approximately 450 nm and a power of 750 mW. The laser was positioned 70 cm from the sample, with a spot area of 0.0022 cm^2 and was activated for 3 minutes, followed by a 3-minute period during which it was turned off. Temperature measurements were taken at the contact point between the thermocouple and the sample during both the laser ON and OFF phases.

3. Results and discussion

3.1. Structural and morphological studies

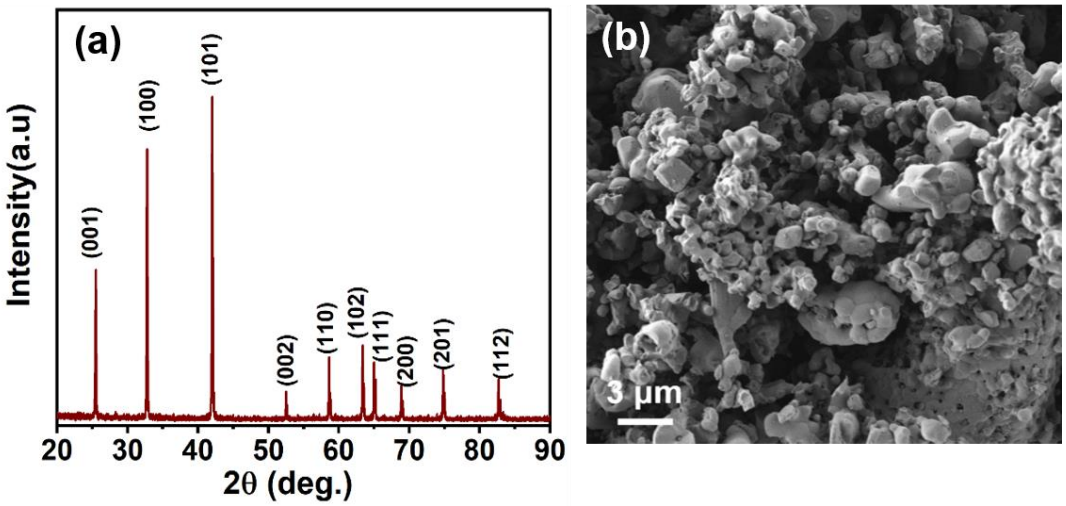

Figure 1. (a) XRD pattern; (b) FESEM image of bulk HfB_2 powder sample

The structural and phase purity studies of the bulk HfB_2 powder were performed based on the X-Ray diffraction data. The XRD pattern shown in Figure 1 (a), confirmed the hexagonal crystalline structure of HfB_2 with ten major peaks at 25.48^O, 32.77^O, 42.04^O, 52.53^O, 58.61^O, 63.38^O, 65.02^O, 68.88^O, 74.83^O and 82.66^O which correspond to the (001), (100), (101), (002), (110), (102), (111), (200), (201) and (112) crystal planes respectively in accordance with ICDD No. 00-038-1398. The unit cell parameters a = 3.143 Å and c = 3.487 Å calculated from the XRD data (Calculations as shown in the Supplementary Information) are in close agreement with the lattice parameter values of a = 3.142 Å and c = 3.476 Å reported in ICDD No. 00-038-1398. The absence of impurity peaks verified the purity of the HfB_2 powder.

The morphological studies of HfB_2 powder were carried out using FESEM. Examination of SEM images depicted in Figure 1 (b) displayed irregular shaped, grainy particles having size distribution ranging from a few hundred nanometers to several micrometers.

3.2. Optical studies

UV-Vis Diffuse Reflectance spectroscopy (UV-DRS) was used to analyse the optical absorption of HfB_2 powder samples as shown in Figure 2 (a). The spectrum demonstrates that the HfB_2 powder sample has a broad absorption in the UV-Vis range with maximum absorption at 420 nm. The photoluminescence spectra, depicted in Figure

2 (b), of HfB_2 were measured from 250 to 550 nm in increments of 25 nm at various excitation wavelengths. The PL spectra indicate that the sample has no emission when compared to the background noise. Based on the optical studies, the material demonstrates a broad band absorption spectrum indicating its ability to absorb light across a wide range of wavelengths. Despite this extensive absorption capability, the material exhibits weak photoluminescence, suggesting that a significant portion of the absorbed energy is not re-emitted as light. This weak photoluminescence points to the possibility of non-radiative processes playing a dominant role in the relaxation of excited electrons within the material (Dovrat *et al*., 2004; Wang *et al*., 2019).

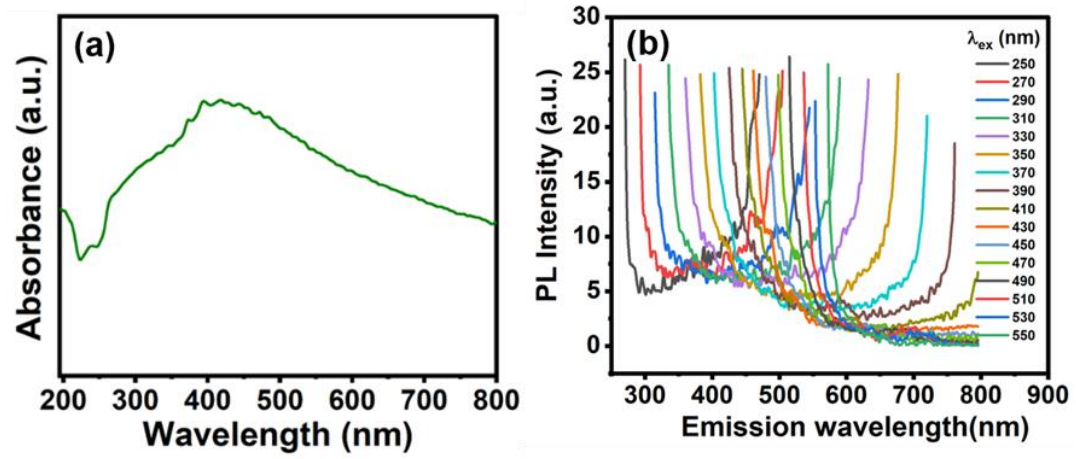

Figure 2. (a) The optical absorption spectra of the HfB_2 powder sample using Diffuse Reflectance Spectroscopy; (b) Photoluminescence (PL) spectra of the HfB_2 powder sample collected at various excitation wavelengths ranging from 250 nm to 550 nm in steps of 25 nm

3.3. Photothermal studies

To evaluate the light-to-thermal conversion efficiency of HfB_2 powder, an investigation of its photothermal properties was conducted by irradiating the sample with a 450 nm continuous-wave blue laser, chosen for its notable absorption characteristics. The laser was operated at a constant intensity of 3 W/cm^2. As detailed in the previous sections, the experimental setup involved a K - type thermocouple connected to the aluminium foil on which the sample is uniformly spread to monitor temperature changes over time. In the absence of light irradiation, the sample remained at room temperature. However, when the laser was activated, it induced a significant heat release within the sample. This led to a rapid increase in temperature, reaching a stable value of approximately 110 °C within about 14.4 seconds, as illustrated in Figure 3 (a).

After the laser was turned off, the sample's temperature decreased back to room temperature, with a reset time of approximately 90 seconds. The material's stability under intense laser irradiation was assessed by performing cyclical ON-OFF experiments, as illustrated in Figure 3 (b). These experiments validated the reproducibility and consistency of the as-generated heat, confirming that the photo-to-heat transduction efficiency of the material remained stable across multiple cycles. The laser power density of the laser beam was altered with neutral density filters, enabling a thorough examination of how the photothermal response varied with different light intensities, as illustrated in Figure 3 (c). The analysis revealed a linear correlation between the light irradiation via generated temperature and the laser intensity, depicted in Figure 3 (d). This finding

underscores that the photothermal effect observed in HfB_2 powder is an intrinsic property of the material, rather than being influenced by external factors or other signals. The temperature reached a peak of approximately 110 °C at a photon flux of about 3 W/cm^2, corresponding to a conversion efficiency of nearly 60 % (Calculations as shown in the Supplementary Information). These results collectively confirm the effectiveness of HfB_2 bulk powder as a highly efficient and stable photothermal agent capable of exhibiting consistent performance which is reproducible.

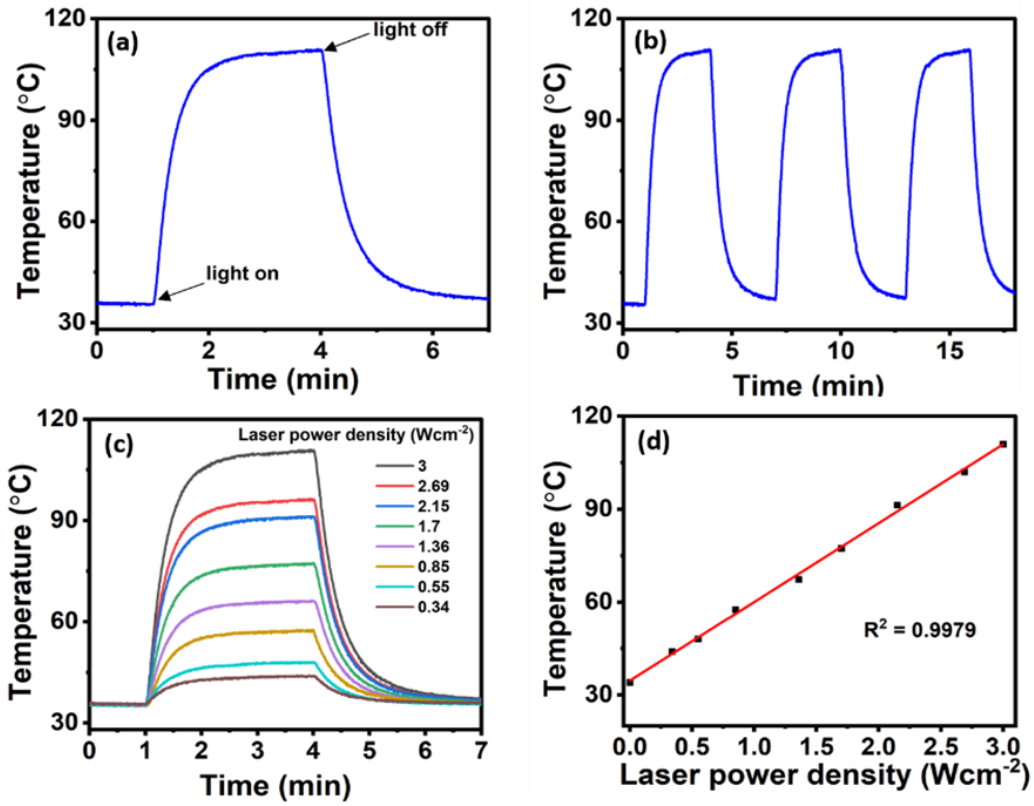

Figure 3. (a) The heating and cooling curves of HfB_2 in powder form;
(b) cyclic tests of photothermal transformation of HfB_2 in powder form at a power density of 3 W/cm^{-2};
(c) heating and cooling curves of HfB_2 in powder form at different power densities of the laser;
(d) the temperature trace of the HfB_2 powder sample with different power densities

4. Conclusion

This study demonstrates the photo-to-heat transduction capability of commercially procured bulk HfB_2 powder, utilised without any further purification or modification, on exposure to continuous wave blue laser beam. The material's extensive absorption throughout the UV-vis spectrum and its minimal photoluminescence facilitates this transduction process. Our results reveal an impressive light-to-heat conversion efficiency of approximately 60 %, coupled with outstanding thermal, chemical and optical stability even under intense laser irradiation. These attributes make HfB_2 powder a viable alternative to conventional nanoscale photothermal agents, whose utilization typically involves complex fabrication processes and difficulties in recovery. Thus, this study suggests a promising shift towards more practical and cost-effective photothermal solutions.

References

Chen, M., He, Y., Zhu, J. & Kim, D.R. (2016). Enhancement of photo-thermal conversion using gold nanofluids with different particle sizes. *Energy Conversion and Management*, 112, 21-30. https://doi.org/10.1016/j.enconman.2016.01.009

Cheng, P., Wang, D. & Schaaf, P. (2022). A review on photothermal conversion of solar energy with nanomaterials and nanostructures: From fundamentals to applications. *Advanced Sustainable Systems, 6*(9), 2200115. https://doi.org/10.1002/adsu.202200115

Das, S., Sozal, M.S.I., Li, W. & John, D. (2023). Ultra-high-temperature ceramic coatings ZrC, ZrB_2, HfC and HfB_2. Springer International Publishing. https://doi.org/10.1007/978-3-031-40809-0_14

Dovrat, M., Goshen, Y., Jedrzejewski, J., Balberg, I. & Sa'ar, A. (2004). Radiative versus nonradiative decay processes in silicon nanocrystals probed by time-resolved photoluminescence spectroscopy. *Physical Review B, 69*(15), 155311. https://doi.org/10.1103/PhysRevB.69.155311

Estelrich, J., Busquets, M.A. (2018). Iron oxide nanoparticles in photothermal therapy. *Molecules, 23*(7), 1567. https://doi.org/10.3390/molecules23071567

Hong, J., Xu, C., Deng, B., Gao, Y., Zhu, X., Zhang, X. & Zhang, Y. (2022). Photothermal chemistry based on solar energy: From synergistic effects to practical applications. *Advanced Science, 9*(3), 2103926. https://doi.org/10.1002/advs.202103926

Huang, H.C., Rege, K. & Heys, J.J. (2010). Spatiotemporal temperature distribution and cancer cell death in response to extracellular hyperthermia induced by gold nanorods. *ACS Nano, 4*(5), 2892-2900. https://doi.org/10.1021/nn901884d

Huang, X., El-Sayed, M.A. (2010). Gold nanoparticles: Optical properties and implementations in cancer diagnosis and photothermal therapy. *Journal of Advanced Research, 1*(1), 13-28. https://doi.org/10.1016/j.jare.2010.02.002

Huang, X., El-Sayed, M.A. (2011). Plasmonic photo-thermal therapy (PPTT). *Alexandria Journal of Medicine, 47*(1), 1-9. https://doi.org/10.1016/j.ajme.2011.01.001

Huang, X., Zhang, W., Guan, G., Song, G., Zou, R. & Hu, J. (2017). Design and functionalization of the nir-responsive photothermal semiconductor nanomaterials for cancer theranostics. *Accounts of Chemical Research, 50*(10), 2529-2538. https://doi.org/10.1021/acs.accounts.7b00294

Jiang, R., Cheng, S., Shao, L., Ruan, Q. & Wang, J. (2013). Mass-based photothermal comparison among gold nanocrystals, PbS nanocrystals, organic dyes and carbon black. *The Journal of Physical Chemistry C, 117*(17), 8909-8915. https://doi.org/10.1021/jp400770x

John, S.K., John, D., Bijoy, N., Chathanathodi, R. & Anappara, A.A. (2017). Magnesium diboride: An effective light-to-heat conversion material in solid-state. *Applied Physics Letters, 111*(3), 033901. https://doi.org/10.1063/1.4994154

Johnson, R.J.G., Haas, K.M. & Lear, B.J. (2015). Fe_3O_4 nanoparticles as robust photothermal agents for driving high barrier reactions under ambient conditions. *Chemical Communications, 51*(2), 417-420. https://doi.org/10.1039/C4CC07966C

Kim, M., Lee, J.H. & Nam, J.M. (2019). Plasmonic photothermal nanoparticles for biomedical applications. *Advanced Science, 6*(17), 1900471. https://doi.org/10.1002/advs.201900471

Lawson, J.W., Bauschlicher Jr, C.W. & Daw, M.S. (2011). Ab initio computations of electronic, mechanical and thermal properties of ZrB_2 and HfB_2. *Journal of the American Ceramic Society, 94*(10), 3494-3499. https://doi.org/10.1111/j.1551-2916.2011.04649.x

Liu, H., Shi, L., Zhang, Q., Qi, P., Zhao, Y., Meng, Q., Feng, X., Wang, H. & Ye, J. (2021). Photothermal catalysts for hydrogenation reactions. *Chemical Communications, 57*(11), 1279-1294. https://doi.org/10.1039/D0CC07144G

Ma, T., Zhu, P. & Yu, X. (2021). Progress in functional studies of transition metal borides. *Chinese Physics B, 30*(10), 108103. https://cpb.iphy.ac.cn/EN/abstract/abstract124017.shtml

Salafi, T., Zeming, K.K. & Zhang, Y. (2017). Advancements in microfluidics for nanoparticle separation. *Lab on a Chip, 17*(1), 11-33. https://doi.org/10.1039/C6LC01045H

Walsh, T., Lee, J. & Park, K. (2015). Laser-assisted photothermal heating of a plasmonic nanoparticle-suspended droplet in a microchannel. *Analyst, 140*(5), 1535-1542. https://doi.org/10.1039/C4AN01750A

Wang, Y., Peng, Q., Liang, H., Brik, M.G., Suchocki, A., Wang, Y., Peng, Q., Liang, H., Brik, M.G. & Suchocki, A. (2019). $^3P_0 \rightarrow {}^1D_2$ non-radiative relaxation control via IVCT state in Pr^{3+}-doped $Na_2Ln_2Ti_3O_{10}$ (Ln=La, Gd) micro-crystals with triple-layered perovskite structure. *Journal of Luminescence*, 213, 510-518. https://eurekamag.com/research/080/904/080904297.php

Wu, X., Chen, G. Y., Owens, G., Chu, D., Xu, H., Wu, X., Chen, G. Y., Owens, G., Chu, D. & Xu, H. (2019). Photothermal materials: A key platform enabling highly efficient water evaporation driven by solar energy. *Materials Today Energy*, 12, 277-296. https://eurekamag.com/research/086/621/086621238.php

Wuchina, E., Opeka, M., Causey, S., Buesking, K., Spain, J., Cull, A., Routbort, J. & Guitierrez-Mora, F. (2004). Designing for ultrahigh-temperature applications: The mechanical and thermal properties of HfB_2, HfC_x, HfN_x and αHf(N). *Journal of Materials Science, 39*(19), 5939-5949. https://doi.org/10.1023/B:JMSC.0000041690.06117.34

Yamamoto, Y., Tokonami, S. & Iida, T. (2019). Surfactant-controlled photothermal assembly of nanoparticles and microparticles for rapid concentration measurement of microbes. *ACS Applied Bio Materials, 2*(4), 1561-1568. https://doi.org/10.1021/acsabm.8b00838

Yao, J., Zheng, Z. & Yang, G. (2018). Layered tin monoselenide as advanced photothermal conversion materials for efficient solar energy-driven water evaporation. *Nanoscale, 10*(6) 2876-2886. https://doi.org/10.1039/C7NR09229F

Yu, C., Xu, L., Zhang, Y., Timashev, P.S., Huang, Y. & Liang, X.J. (2020). Polymer-based nanomaterials for noninvasive cancer photothermal therapy. *ACS Applied Polymer Materials, 2*(10), 4289-4305. https://doi.org/10.1021/acsapm.0c00704

Zhang, J., Tang, T., Yang, R., Wang, G., Ye, K.H. & Shi, J. (2024). Photothermal effect and application of photothermal materials in photocatalysis and photoelectric catalysis. *Microstructures*, 4, 2024008. https://doi.org/10.20517/microstructures.2023.51

Zhang, X., Luo, X., Han, J., Li, J. & Han, W. (2008). Electronic structure, elasticity and hardness of diborides of zirconium and hafnium: First principles calculations. *Computational Materials Science, 44*(2), 411-421. https://doi.org/10.1016/j.commatsci.2008.04.002

Zhou, J., Li, X., Chen, W., Cui, R. & Wu, X. (2022). Investigation on the photothermal performance of carbon quantum dots nanofluid with high-stability. *Diamond and Related Materials*, 128, 109233. https://doi.org/10.1016/j.diamond.2022.109233